Downscaling and Calibration Analysis of Precipitation Data in the Songhua River Basin Using the GWRK Model and Rain Gauges

Bo Zhang, Chuanqi Liu, Zhijie Zhang, Shengqing Xiong, Wanchang Zhang, Zhenghao Li, Bangsheng An, and Shuhang Wang

***Abstract*—Obtaining high-quality precipitation data with both high spatial and temporal resolution is imperative for hydrological and meteorological research. However, the coarse resolution and uncertain data quality of most satellite data, coupled with sparse rain gauge station (RGS), limit their direct applicability in scientific research. Downscaling satellite data, particularly in conjunction with RGS, proves to be an effective approach to overcome this challenge. In this study, we utilize the geographically weighted regression kriging model to downscale global precipitation measurement IMERG monthly precipitation data from 2001 to 2020. Leveraging spatially heterogeneous relationships with digital elevation model, slope, land surface temperature, and soil moisture in the Songhua River Basin in Northeast China, we enhance the spatial resolution from 0.1° to 1 km, initially achieving a 1.4% increase in data accuracy, with a CC value of 0.966. Subsequently, employing the daily fraction method, the downscaled precipitation data are disaggregated to the daily scale and calibrated by merging RGS using the geographical difference analysis method. The outcome is high-quality daily precipitation data with both high spatial resolution and accuracy (CC = 0.818, RMSE = 3.188, and ME = 0.086). An analysis of the annual variation of precipitation in the Songhua River Basin over the past two decades reveals an increasing trend. Spatially, the average annual precipitation variation rate in the basin increases from the middle to both ends, with the increasing trend gradually decreasing from south to north. The proposed approach provides a practical solution for enhancing the spatiotemporal scale of satellite data, improving data quality, and addressing the sparse distribution of RGS.**

***Index Terms*—Downscaling, geographically weighted regression kriging (GWRK), precipitation, Songhua River Basin.**

I. Introduction

THE primary scientific challenge in hydrology and water environment research currently revolves around the uncertainty of meteorological elements [1]. Precipitation, a pivotal meteorological indicator, profoundly influences global climate patterns and the Earth's biomass energy cycle system with its temporal and spatial distribution [2], [3]. Consequently, high-quality precipitation data are indispensable for various environmental studies, including flood forecasting, drought monitoring, and watershed hydrological research [4], [5], [6], [7].

Acquiring high spatial and temporal resolution precipitation data remains a significant challenge despite its importance [8]. Precipitation, as a complex natural phenomenon, exhibits considerable variability in both time and space [9]. Typically, precipitation data can be sourced from rain gauges, satellite quantitative precipitation estimates, radar precipitation estimates, and model forecasts or reanalysis products [10], [11]. Traditional methods for obtaining spatially continuous and accurate precipitation data rely primarily on the spatial interpolation of rain gauge data [12], such as inverse distance weighting (IDW) [13] and kriging interpolation methods. Due to the limited number of rain gauges, the precipitation measured at one site is often used to represent an area of tens to hundreds of square kilometers, which may not be accurate, especially in alpine mountainous regions [14]. The limited number and spatial distribution of rain gauges introduce substantial uncertainty in the interpolation results [15]. Additionally, considering the spatial heterogeneity of precipitation, using point values to represent large-scale precipitation is often inaccurate [16].

Alternatively, satellite precipitation data, such as those from the global precipitation climatology project, global satellite mapping of precipitation, tropical rainfall measuring mission (TRMM), and global precipitation measurement (GPM) product datasets, have gained popularity in scientific research due to

Manuscript received 26 March 2024; revised 22 May 2024 and 13 June 2024; accepted 26 June 2024. Date of publication 5 July 2024; date of current version 24 July 2024. This work was supported by the Major Science and Technology Project of Ministry of Water Resources under Grant SKS-2022008. *(Bo Zhang and Chuanqi Liu are co-first authors.) (Corresponding author: Zhijie Zhang.)*

Bo Zhang and Shuhang Wang are with the National Engineering Laboratory for Lake Pollution Control and Ecological Restoration, Chinese Research Academy of Environmental Sciences, Beijing 100012, China (e-mail: zhangbo@craes.org.cn; wangsh@craes.org.cn).

Chuanqi Liu, Zhenghao Li, and Bangsheng An are with the Key Laboratory of Digital Earth Science, Aerospace Information Research Institute, Chinese Academy of Sciences, Beijing 100094, China, also with the International Research Center of Big Data for Sustainable Development Goals, Beijing 100094, China, and also with the University of Chinese Academy of Sciences, Beijing 100049, China (e-mail: liuchuanqi20@mails.ucas.ac.cn; lizhenghao21@mails.ucas.ac.cn; anbangsheng21@mails.ucas.ac.cn).

Zhijie Zhang is with the Department of Environment and Society, Quinney College of Natural Resources, Utah State University, Logan, UT 84322 USA, and also with the Natural Resources Aero-Geophysical and Remote Sensing Centre, China Geological Survey Bureau, Beijing 84322, China (e-mail: zhijiezhang@arizona.edu).

Shengqing Xiong is with the Natural Resources Aero-Geophysical and Remote Sensing Centre, China Geological Survey Bureau, Beijing 100083, China (e-mail: xsqagrs@126.com).

Wanchang Zhang is with the Key Laboratory of Digital Earth Science, Aerospace Information Research Institute, Chinese Academy of Sciences, Beijing 100094, China, and also with the International Research Center of Big Data for Sustainable Development Goals, Beijing 100094, China (e-mail: zhangwc@radi.ac.cn).

Digital Object Identifier 10.1109/JSTARS.2024.3424349

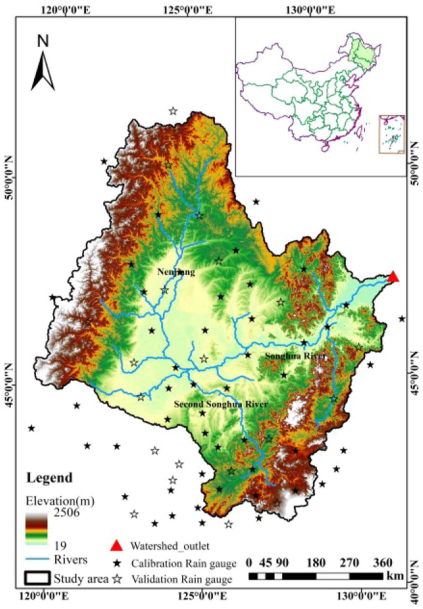

Fig. 1. Location of Songhua River Basin and the rain gauges in and around the study area.

their wide spatial coverage and ease of acquisition [17], [18], [19], [20]. However, the quality of satellite precipitation data is challenged by inversion algorithms, terrain complexity, and sensor sensitivity, which lead to uncertainties in data accuracy [21]. Moreover, the spatial resolution of satellite products is often too coarse for local watershed hydrological modeling and meteorological research [22]. To address these issues, spatial downscaling and calibration procedures are essential before applying satellite precipitation data in hydrological and meteorological models [23], [24], [25].

Relevant studies have shown that the precipitation downscaling calibration scheme of extreme gradient boosting (XGBoost_DC), which integrates rain gauge data, can enhance the spatial resolution and accuracy of satellite precipitation extremes and capture some small-scale heavy rainfall processes [26]. Additionally, researchers have proposed an attention-based convolutional network for spatial precipitation downscaling and a geointelligent deep belief network for surface precipitation-satellite fusion, achieving promising results in China [27].

Traditional statistical downscaling methods, including exponential regression, multiple linear regression, random forest models, and artificial neural network models, assume spatial constancy in the relationship between precipitation and environmental variables, overlooking the spatial heterogeneity and scale-dependent nature of this relationship [28], [29], [30]. GWR model has emerged as a preferred method, considering spatial and temporal variability in precipitation relationships [6], [31]. Several studies have highlighted the efficacy of GWR in handling spatial heterogeneity and temporal diversity, outperforming other downscaling methods [22], [31].

In this context, this study investigates the complex spatial relationships between IMERG precipitation data and various environmental factors, including digital elevation model (DEM), slope, soil moisture, and land surface temperature (LST). A geographically weighted regression kernel (GWRK) model was developed by employing rain gauge observations and satellite precipitation data. Monthly scale IMERG precipitation data are downscaled from the original 0.1° to a finer 1 km. The high-resolution daily precipitation estimates are obtained using the monthly fraction method. The downscaling process is calibrated and validated using the geographical difference analysis (GDA) method, augmented with rain gauge data to produce high-resolution, accurate daily precipitation maps covering the Songhua River basin between 2001 and 2020.

The rest of this article is organized as follows. Section II analyzes the geographical and climatic conditions of the study area. Section III introduces the various datasets and rain gauge data used in the research. Section IV introduces the methods and model principles adopted in the study. In Section V, the downscaling and calibration results at different time scales are analyzed. In Section VI, we discuss the application of the GWRK model, sources of uncertainty in the model, and directions for future downscaling research. Finally, Section VII concludes this article.

II. Study Area

The study area, the Songhua River basin, as shown in Fig. 1, situated in the northern part of Northeast China, stands as the largest tributary of the Heilongjiang River in China. Encompassing geographical coordinates between 41°42′–51°38′N and 119°52′–132°31′E, the expansive Songhua River Basin covers an area of 557 825 km^2, constituting 30.2% of the total Heilongjiang River Basin [32]. The basin boasts diverse landform features, with the Wanda Mountains to the east, the Changbai Mountains to the southeast, and mountainous and hilly terrain in the southwest, delineating the watershed of the Songhua River and Liaohe River basins. To the west and north, the Greater and Lesser Khingan Mountains, respectively, contribute to the basin's topography [33]. The central Songnen Plain, characterized by its rich population concentration and agricultural productivity, features numerous lakes and wetlands.

The Songhua River Basin experiences a north temperate monsoon climate, marked by warm and rainy summers, cold and dry winters, and notable temperature variations throughout the year [34]. The annual average temperature ranges between 3 and 5 °C, with July recording the highest temperatures, reaching a daily average of 20–25 °C and occasionally exceeding 40 °C. Conversely, January exhibits the lowest temperatures, with monthly averages dropping below −20 °C [35]. The basin receives an annual average precipitation of approximately 500 mm, varying across the region, with the southeastern mountainous areas receiving 700–900 mm and the relatively arid western region registering around 400 mm [36].

Known for its intricate water system, the Songhua River Basin is endowed with abundant water resources, boasting an annual runoff of 76.2 billion m^3. This unique combination of geographical features and climatic conditions makes the Songhua River Basin an ideal focus for the investigation into precipitation patterns through the application of the GWRK model and rain gauge data, as shown in Fig. 1.

III. Material

A. GPM_IMERG Data

The GPM mission, an international satellite network launched on 28 February 2014, provides cutting-edge global precipitation data, building upon the TRMM [37]. Equipped with the first spaceborne Ku/Ka Doppler dual-frequency precipitation radar and multichannel GPM microwave imager, this satellite, jointly developed by NASA and the Japan Aerospace Exploration Agency [38], significantly enhances precipitation detection capabilities [39]. Compared with TRMM data, GPM data demonstrate improved measurement capabilities for light rain, solid precipitation, and precipitation particles, showcasing superior performance [40], [41]. Monthly precipitation data in this study are derived from GPM-3IMERGM precipitation data with a spatial resolution of 0.1°, available publicly.[1]

B. Environment Variable Data

The 90-m resolution DEM data utilized originate from the Shuttle Radar Topography Mission Project, sponsored by the National Geospatial-Intelligence Agency and NASA. Slope data, created using ArcGIS 10.5 based on DEM data, complement this dataset. MOD11A2 LST data, acquired from the NASA Land Processes Distributed Activity Archive Center Data, cover the period 2001–2020, presenting eight-day intervals aggregated into monthly averages. Soil moisture data, a 1 km high-quality dataset within China, rely on the China Meteorological Administration's (CMA) ten-layer soil moisture observations. Additional covariates, including ERA5_Land time-series data, leaf area index, and land cover type, obtained through machine learning, contribute to the dataset. These datasets, available on the space–time tripolar environmental big data platform[2] [42], [43], undergo resampling from 90 m and 1 km to 0.1°, aligning with the IMERG data resolution.

C. Rain Gauge Data

Long-term monthly precipitation data derive from the daily rainfall data of 70 CMA rainfall stations.[3] Daily precipitation data accumulate from 20:00 P.M. on the previous day to 20:00 P.M. on the current day, Beijing time, spanning the years 2001–2020. Among these, 50 stations contribute to calibration, while 20 stations serve for validation. The selection of verification and calibration stations involves sorting based on station serial numbers. Verification stations are chosen at regular intervals, ensuring comprehensive coverage across the study area for more effective precipitation data calibration results. Statistical results indicate an average rainfall of 565.5 mm from 2001 to 2020, with 2020 being the wettest year at 722.2 mm and 2001 the driest at 408.3 mm. The geographical distribution of basin sites is illustrated in Fig. 1.

[1][Online]. Available: https://pmm.nasa.gov/data-access/downloads/gpm
[2][Online]. Available: https://doi.org/10.11888/Terre.tpdc.272415
[3][Online]. Available: http://data.cma.cn

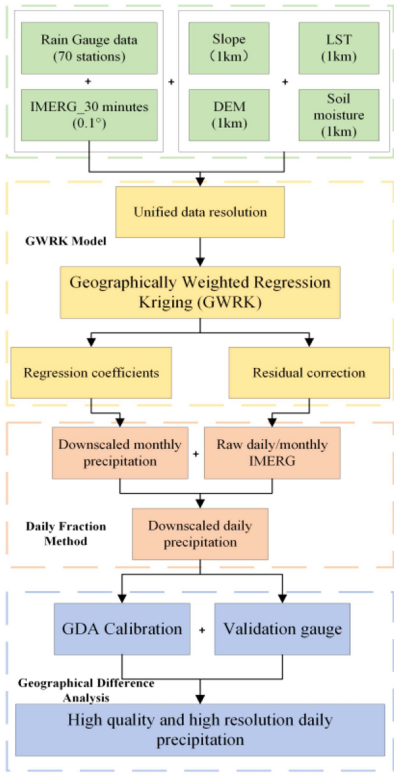

Fig. 2. Flowchart illustrating the integrated downscaling process, merging rain gauge data with the GWRK model, employed to generate high-resolution (1 km × 1 km) precipitation data in the context of this study.

IV. Methods

This study comprises two main phases.

Monthly Scale Processing and Analysis: In this initial phase, a GWR model is developed, incorporating four geographic and environmental factors to facilitate precipitation downscaling. Geographic factors, such as the DEM and slope, along with environmental factors, such as LST and soil moisture data, are resampled to the original resolution of the IMERG data (0.1°). Simultaneously, coarse-resolution environmental factors and precipitation data are transformed into monthly datasets. Utilizing these datasets, the GWR model generates fine-resolution monthly precipitation data (1 km). The model produces residuals at coarse resolution, necessitating kriging interpolation to map these residuals to the downscaled resolution. The resulting interpolated residual map is then combined with the regression prediction map, yielding the final GWRK downscaling outcome.

Daily Processing: In the second phase, precipitation data undergo further processing at the daily scale. The GDA method is applied to calibrate daily precipitation data in conjunction with calibration site data. Subsequently, the quality of the daily calibration data is evaluated using verification sites. This process concludes with the acquisition of the final daily downscaled precipitation dataset for the Songhua River Basin.

Fig. 2 illustrates the flowchart of the integrated downscaling process, showcasing the combination of rain gauges with the GWRK model to generate high-resolution (1 km × 1 km) precipitation data in the present study.

A. GWRK Model

GWR is a local regression model first proposed by Brunsdon et al. [44]. Since it assumes that regression coefficients vary with geographical location, it has been widely used to study the dynamic and scale-dependent characteristics between predictors and explanatory factors [45], [46]. Precipitation is one of the most typical research indicators in meteorological research, and its spatial heterogeneity is its most important feature [47]. Therefore, the geographically weighted regression model can perform better in precipitation downscaling [48]. The model is expressed as follows:

$$Y_j = \beta_0 (u_j, vj) + \sum_{i=1}^{n} \beta_i (u_j, vj) X_{ij} + \varepsilon_j \quad (1)$$

where (u_j, vj) is the latitude and longitude coordinates of the jth point; $\beta_0(u_j, vj)$ is the intercept at point j, which is the estimated value of the local constant term; $\beta_i(u_j, vj)$ is the regression coefficient at point j, which is the local estimate of the coefficient of each variable; ε_j is the residual at point j, which represents the difference between the jth observed value and the predicted value of the dependent variable; Y_j is the jth dependent variable (satellite precipitation) observations; X_{ij} is the ith explanatory variable at location j; n is the number of explanatory variables (elevation, slope, LST, and soil moisture)

$$\beta (u_j, v_j) = \left(X^T (W (u_j, v_j)) X\right)^{-1} X^T W (u_j, v_j) Y \quad (2)$$

where $\beta(u_j, v_j)$ represents the local coefficient to be estimated at position (u_j, v_j); X and Y are the vectors of explanatory variables and dependent variables, respectively; and $W(u_j, v_j)$ is the weight matrix. This is the main step in building a GWR model and greatly affects the final accuracy of the model [49]. Currently, there are several methods that can be used to determine the weight matrix [50]. In this research, the Gaussian function was selected to determine the weight

$$W_{ij} = \exp\left(-(d_{ij}/b)^2\right) \quad (3)$$

where W_{ij} is the weight of the observation at position j used to estimate the coefficient at position i; d_{ij} is the Euclidean distance between i and j; and b is the basis width of the kernel function. In order to reduce the computational cost, the Gaussian function defined above can be replaced by a bisquare function. Most verification methods for the basis width of kernel functions use the modified Akaike information criterion (AICc).

$$\mathrm{AICc} = 2n\ln(\hat{\sigma}) + n\ln(2\pi) + n\left(\frac{n + \mathrm{tr}(S)}{n - 2 - \mathrm{tr}(S)}\right) \quad (4)$$

where n is the number of the sample size, $\hat{\sigma}$ is the estimate of the standard deviation of the residuals, and $tr(S)$ represents the trace of the hat matrix.

For the GWRK method, the ordinary kriging (OK) method needs to be used to interpolate the residuals in GWR to the target resolution (1 km), and the interpolated residual map is added to the regression prediction map to obtain the GWRK map.

B. Daily Fraction Method

The daily fraction method is based on the fact that the daily fraction is more accurate than the absolute value of the uncalibrated raw GPM precipitation data, and subsequent experiments also verified this assumption [2], [22]. The expression of the daily fraction method is given as follows:

$$\mathrm{GPM}_{\mathrm{daily}} = \left(\frac{\mathrm{OriGPM}_i^{0.1^\circ}}{\sum_{i=1}^{n} \mathrm{OriGPM}_i^{0.1^\circ}}\right) \mathrm{GPM}_{\mathrm{month\_GWRK}}^{1\,\mathrm{km}}. \quad (5)$$

Among them, $\mathrm{OriGPM}_i^{0.1^\circ}$ represents the original daily precipitation of the ith day; n represents the corresponding number of days in the month; and $\mathrm{GPM}_{\mathrm{month\_GWRK}}^{1\,\mathrm{km}}$ represents the corresponding monthly precipitation after GWRK downscaling. It should be noted that the spatial scale of the precipitation fraction obtained based on the daily fraction method is 0.1° and needs to be interpolated to 1 km. The interpolated precipitation fraction is multiplied by the downscaled monthly precipitation to obtain high-resolution daily precipitation estimates.

C. Geographical Difference Analysis

In order to further improve the accuracy of downscaled precipitation data, this study also uses GDA combined with rain gauge data to further calibrate the downscaled data [51], [52]. The formula is given as follows:

$$P\mathrm{cal}(x) = P_{\mathrm{down}}^{1\,\mathrm{km}}(x) + \sum_{i=1}^{n} \theta_i \left(P_{\mathrm{obs}}(x_i) - P_{\mathrm{down}}^{1\,\mathrm{km}}(x_i)\right) \quad (6)$$

where $P\mathrm{cal}(x)$ is the final calibrated precipitation at target point x; $P_{\mathrm{down}}^{1\,\mathrm{km}}(x_i)$ is the downscaled precipitation value at location x_i; $P_{\mathrm{obs}}(x_i)$ is the precipitation observed by the rain gauge at location x_i; and n is the number of observations near the target point x used in the interpolation. θ_i is the weight at position x_i, and the estimated variance is minimized by constraints on the weights. In addition, the residual between the observed precipitation at the target point and the reduced precipitation needs to be interpolated to 1 km using the OK method, and then fused with the downscaled data to obtain the final calibration downscaled data.

D. Validation

Monthly GPM-IMERG precipitation estimates were downsized for the period 2001–2020. The downscaled precipitation estimates were calibrated and evaluated using ground observation data from 70 weather stations. Four statistical indicators were selected for validation: correlation coefficient (CC), mean error (ME), and root-mean-square error (RMSE). CC represents the strength of correlation between surface observations and precipitation estimates. ME is used to evaluate the accuracy of forecasts or models, which represents the average value of the difference between the observed and predicted values. RMSE represents the size of the error estimate. Their calculation formula is given as follows:

$$\mathrm{CC} = \frac{\sum_{i=1}^{n} (M_i - \bar{M})(P_i - \bar{P})}{\sqrt{\sum_{i=1}^{n} (M_i - \bar{M})^2 (P_i - \bar{P})^2}} \quad (7)$$

TABLE I
QUALITY OF RAW SATELLITE PRECIPITATION DATA AT DAILY AND MONTHLY SCALES IN THE SONGHUA RIVER BASIN FROM 2001 TO 2020

	CC	RMSE	ME
Monthly	0.952	20.302	6.985
Daily	0.733	4.077	0.229

$$\mathrm{ME} = \frac{1}{n}\sum_{i=1}^{n}(P_i - M_i) \tag{8}$$

$$\mathrm{RMSE} = \sqrt{\frac{\sum_{i=1}^{n}(P_i - M_i)^2}{n}} \tag{9}$$

where M_i and P_i are the observed precipitation and estimated precipitation at the ith weather station location, respectively; $\bar{M}$ and $\bar{P}$ represent the mean values of M_i and P_i, respectively; and n is the number of weather stations used for verification.

V. RESULT

A. Data Accuracy of Raw GPM Satellite Precipitation Data

The efficacy of the GWR model hinges significantly on the quality of the original resolution precipitation data [22], [48]. Thus, prior to downscaling, an assessment of the satellite precipitation data's quality is imperative. In this study, precipitation data at both monthly and daily scales for the Songhua River Basin from 2001 to 2020 were downscaled and calibrated. The basin is equipped with 70 rain gauges, and satellite data were acquired by aggregating half-hour raw satellite readings based on Beijing time. The table below illustrates the quality analysis of the raw satellite precipitation data.

For the daily scale data, CC, ME, and RMSE are 0.733, 0.229, and 4.077, respectively. For the monthly scale data, CC, ME, and RMSE are 0.952, 6.985, and 20.302 (see Table I). The ME value indicates a general overestimation of precipitation in the basin by the original IMERG data. Despite this, considering the overall quality of the original precipitation data, this study asserts that the GPM satellite data meet the requisite standards for precipitation downscaling using the GWRK model.

B. Quality Correlation Analysis of Environmental Explanatory Variables

In this study, DEM, slope, soil moisture, and LST serve as auxiliary variables for constructing the GWRK model. As DEM and slope exhibit minimal variation over the study period, the analysis focuses solely on soil moisture and LST quality. Initially, the accuracy of LST data is verified by comparing it with data from 70 meteorological observation stations and processed MODIS LST data. Subsequently, correlations among LST, soil moisture, and raw satellite precipitation are analyzed, and the results are presented in Fig. 3.

As can be observed that the MODIS LST data exhibit good quality, with a CC value of 0.664 against the ground measurement data. Moreover, the CC diagram illustrates strong correlations among LST, soil moisture data, and original satellite precipitation data. Throughout the study period, the CC values of LST, soil moisture, and original satellite precipitation in the Songhua River Basin were 0.670 and 0.628, respectively.

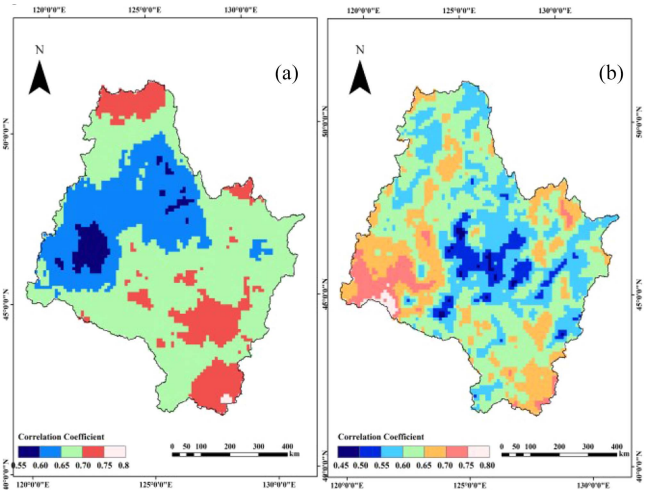

Fig. 3. Spatial distribution of CCs among (a) LST, (b) soil moisture, and satellite precipitation data at the monthly scale from 2001 to 2020.

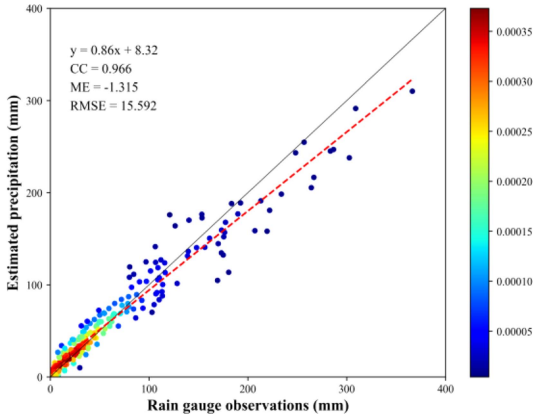

Fig. 4. Scatter plot after downscaling of monthly precipitation data.

Based on the accuracy of the environmental variables and their correlation with precipitation, this study contends that the construction of a GWRK model will yield improved downscaled precipitation results.

C. Analysis of GWRK Model Precipitation Downscaling Results

The GWRK downscaling model, designed to elucidate the spatial heterogeneity relationship between environmental variables and precipitation, has yielded promising outcomes. This is exemplified by the findings, as presented in Fig. 4 and Table II.

Compared with raw precipitation data, the GWRK model has enhanced the accuracy of precipitation data while mitigating RMSE and ME. The downscaled precipitation data exhibit refined spatial distribution characteristics at a resolution of 1 km. Following downscaling, the CC of monthly precipitation data

TABLE II
ACCURACY ANALYSIS BEFORE AND AFTER DOWNSCALING OF MONTHLY PRECIPITATION DATA

	CC	RMSE	ME
Monthly_Raw	0.952	20.302	6.985
Monthly_Down	0.966	15.592	–1.315

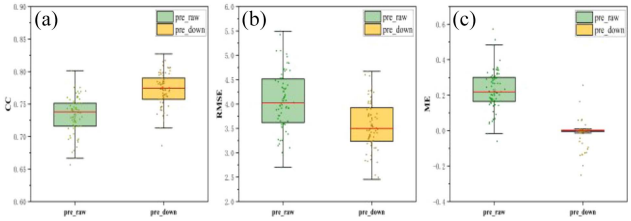

Fig. 5. Boxplots of statistical indicators of downscaled daily precipitation data from 70 rain gauge stations. (a) CC. (b) RMSE. (c) ME.

TABLE III
ACCURACY ANALYSIS BEFORE AND AFTER DOWNSCALING OF DAILY PRECIPITATION DATA

	CC	RMSE	ME
Daily_Raw	0.733	4.077	0.229
Daily_Down	0.772	3.562	–0.012

increased from 0.952 to 0.966, with ME and RMSE decreasing from 6.985 and 20.302 to −1.315 and 15.592, as listed in Table II, respectively. This supports our hypothesis regarding the downscaling effect based on the correlation between explanatory variables and precipitation.

Further comparison with the original data quality reveals an improvement in the quality of satellite data to some extent. Subsequently, we employ the daily fraction decomposition method to disaggregate the downscaled monthly precipitation data to the daily scale, evaluating the GWRK model's downscaling efficacy [2].

Fig. 5 depicts the quality of decomposed daily precipitation data. Relative to the original daily precipitation data, the CC of the monthly precipitation data increased from 0.733 to 0.772, with ME and RMSE decreasing from 0.229 and 4.077 to −0.012 and 3.562, as listed in Table III, respectively. These results indicate the GWRK model's efficacy in handling daily precipitation data as well. However, slight overestimation persists in the downscaling results compared with rain gauge data. Given this, our next step involves integrating rain gauge data to calibrate the daily precipitation data [24].

D. Calibration of Downscaling Results From Fused Rain Gauge Data

The construction of the GWRK downscaling model yielded favorable outcomes on both the monthly and daily scales. However, to address the disparity between satellite precipitation products and actual precipitation, the fusion of rain gauge data with downscaled precipitation data becomes imperative. Out of the 70 available rain gauges, 50 are selected for the calibration group, while the remaining 20 constitute the verification group.

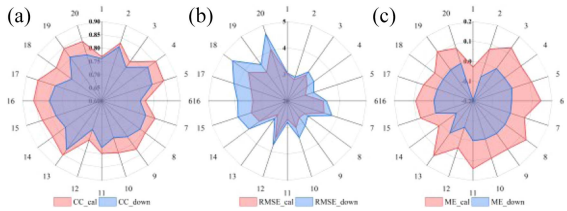

Fig. 6. Radar plots of CC, ME, and RMSE of the observed, downscaled, and calibrated daily precipitation.

TABLE IV
ACCURACY ANALYSIS BEFORE AND AFTER CALIBRATION OF DAILY PRECIPITATION DATA

	CC	RMSE	ME
Daily_Down	0.772	3.562	–0.012
Daily_Cal	0.818	3.188	0.086

Selection of the verification group follows a rule of sorting rain gauges by site number and choosing at regular intervals, ensuring a spatially even distribution of sites in both validation and calibration groups. Given the vastness of the Songhua River basin and the absence of precipitation in some station areas, this study employs GDA in conjunction with the IDW method to integrate the downscaling results and rain gauge data, as shown in Fig. 6.

The results underscore that the calibration process of fused rain gauge data significantly enhances the accuracy of the downscaling outcomes. In comparison with the downscaling results, the CC of the calibrated daily data increased from 0.772 to 0.818 (see Table IV), while the ME and RMSE reduced from −0.012 and 3.562 to 0.086 and 3.188, respectively. These findings emphasize the necessity of further calibration processing of the downscaling results through the integration of rain gauge data.

E. Analysis of Spatial and Temporal Distribution of Precipitation in the Songhua River Basin

The spatial pattern of GWR downscaled monthly average precipitation in the Songhua River Basin, spanning from 2001 to 2020, is illustrated in Fig. 7. Notably, the maximum monthly average precipitation occurs in August, while the minimum is observed in January. Spatially, precipitation increases from northwest to southeast, with concentration in the eastern and southern regions of the basin. This distribution aligns with seasonal patterns, as higher altitude central and northern areas receive less precipitation compared with the lower altitude southeastern regions. The western region, despite its lower altitude, experiences reduced precipitation due to water vapor blockage by the Great Khingan along the east coast. In addition, by comparing the precipitation data before and after downscaling, it can be clearly found that the downscaled data not only have higher data accuracy but also have higher spatial resolution, which can describe the spatial changes of local precipitation in more detail.

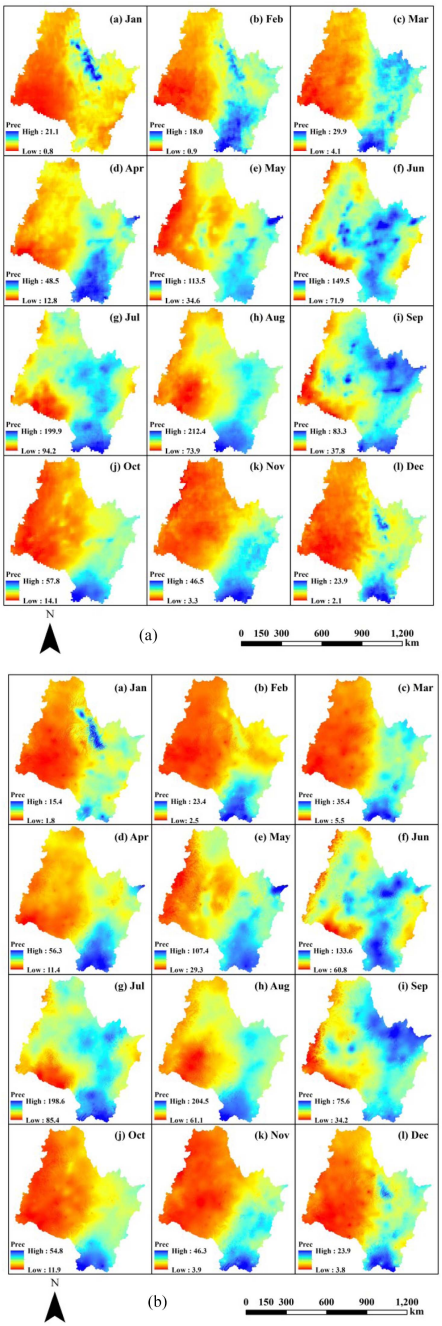

Fig. 7. Spatial distribution of average monthly precipitation in the Songhua River Basin from 2001 to 2020. (a) Represents the original satellite data. (b) Represents the downscaled satellite data.

The spatial and temporal changes in annual average precipitation in the Songhua River Basin are illustrated in Fig. 8. Overall, the basin experiences an increasing trend in annual precipitation without any significant areas of decline. Spatially, the average annual precipitation slope gradually rises from the central region toward both ends, with the increasing trend diminishing from south to north. Temporally, there is a consistent increase in the average annual precipitation, with an annual increment of 10.98 mm/year, reaching an average of 564.95 mm. Compared with the original satellite precipitation data, the multiyear

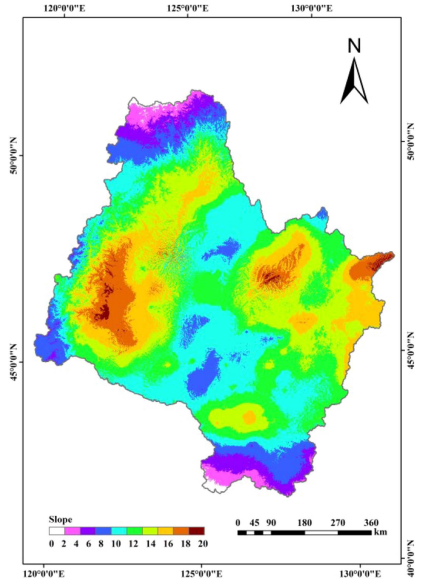

Fig. 8. Spatial distribution of annual precipitation slope changes in the Songhua River Basin from 2001 to 2020.

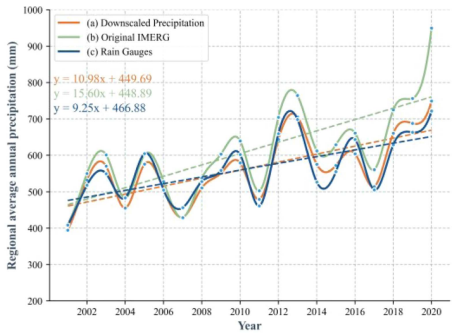

Fig. 9. Change trend of regional average annual precipitation in the Songhua River Basin from 2001 to 2020. (a) Downscaled precipitation. (b) Original IMERG. (c) Rain gauges.

change trend of the downscaled precipitation data is obviously more consistent with the rain gauge data (see Fig. 9).

VI. Discussions

A. Applicability of the GWRK Precipitation Downscaling Model

Traditional approaches to downscale satellite precipitation datasets often assume a spatially constant relationship between precipitation and environmental variables [5], [53]. In contrast, the GWRK model, as employed in this study, considers the spatial heterogeneity relationship between precipitation and various auxiliary variables, showcasing superior performance across diverse regions [24], [54], [55]. Our findings demonstrate that the GWRK downscaling model effectively reduces IMERG monthly scale satellite data from 0.1° to 1 km resolution, concurrently enhancing data quality.

A range of spatial auxiliary variables, including DEM, slope, aspect, NDVI, latitude, and longitude, has been utilized in the GWRK downscaling model by other researchers [8], [28]. In

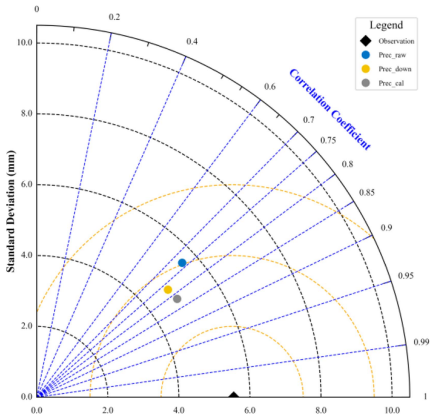

Fig. 10. Taylor plots of original daily precipitation data, downscaled precipitation data, and calibrated downscaled data from 2001 to 2020. "Observation" denotes the rain gauge data.

this study, we comprehensively considered the impact of topographic conditions and environmental factors in the study area, selecting DEM, slope, LST, and soil moisture as spatial auxiliary variables. NDVI was omitted due to concerns about potential linear redundancy and a lag in the spatiotemporal relationship between NDVI and precipitation. Prior to model construction, quality verification and correlation analyses were conducted on the chosen auxiliary variables, all of which exhibited close spatiotemporal correlation with precipitation. This careful selection of environmental variables significantly influenced the satisfactory downscaling results.

Furthermore, the integration of the daily fraction method and the GDA method yielded high-quality daily data based on the downscaled high-precision data, as presented in Fig. 10, further validating the application potential of the GWRK model.

At the same time, comparing the downscaling and calibration results obtained by the GWRK model with other latest precipitation downscaling research methods, the method proposed in this study is still satisfactory. Compared with the transfer deep learning method applied to the Yangtze River Basin in China (CC = 0.715, downscaling to 1 km, daily time scale to 2013) [56], the final downscaled precipitation results provided by the GWRK model have higher data accuracy and the same space resolution and longer time series (CC = 0.818, downscaling to 1 km, daily time scale 2001–2020). Four precipitation downscaling models based on deep learning, including support vector regression, random forest, spatial random forest, and extreme gradient boosting, have been applied in Guangdong, southern China, and have achieved excellent results. The optimal value of the final downscaling result of average annual precipitation is CC = 0.95, which is obtained by the SVR_GDA (support vector regression downscaling calibration) method [57]. The precipitation downscaling method proposed in this study has a determination coefficient of $R^2 = 0.932$ on the monthly scale. However, considering the variations in climate and terrain across different regions, the differences in satellite data sources and downscaling methods used, as well as the sparse distribution of rain gauges, we cannot simply rely on the data quality of the final results to judge the effectiveness of the downscaling methods. Similarly, we can also learn more diverse downscaling methods from the above-mentioned related research articles so that we can choose a more suitable method for our own research according to our actual research needs.

Compared with the above studies, this study selected soil moisture, which is less used in the current study, as one of the downscaling spatial auxiliary variables. After analysis, it was found that soil moisture and precipitation have a strong correlation, which also proves the rationality of studying spatial auxiliary variables. In addition, this study obtained long time-series (20 years) daily high-quality (CC = 0.818) 1 km precipitation data in the study area. The resolution and data quality are significantly improved compared with the original data. At the same time, the data can also be processed into products of different time scales according to different needs, and combined with relevant data, conduct multiscale drought and flood research on the study area. This also reflects the strong application potential of downscaled data in hydrometeorological research.

B. Model Uncertainty and Error Sources

While the precipitation downscaling model based on GWRK offers high-quality long-series precipitation data products at daily and monthly scales, inherent uncertainties persist throughout the downscaling process, potentially influencing the quality of the final precipitation products.

First, satellite-derived precipitation estimates inherently carry spatially varying errors stemming from terrain characteristics, inversion algorithms, and insufficient sensitivity between electromagnetic signals and clouds [58], [59]. Original satellite data may exhibit varying degrees of precipitation overestimation or underestimation in different regions and seasons, thereby impacting the GWRK precipitation downscaling model's ability to achieve higher quality predictions.

Moreover, the selection of environmental variables presents an opportunity for further optimization. Additional environmental variables, such as land use type, coastline distance, cloud properties, wind speed, and roughness, may influence the spatial distribution of precipitation and potentially enhance the accuracy of precipitation downscaling [22], [24].

Finally, systematic errors and uncertainties in rain gauge measurements contribute to potential inaccuracies. Instrument measurement errors, including insufficient recording of wind speed effects, wetting losses, evaporation losses, and underestimation of precipitation, are prevalent [60], [61], [62]. Particularly in high-altitude areas, such errors are more pronounced [63]. Situated in the northernmost region of China (41°N–51°N), the Songhua River Basin experiences an annual average temperature of 3–5 °C, with temperatures below −20 °C in January. These harsh conditions amplify the systematic measurement errors of rain gauges in the basin.

C. Research Prospects

Future endeavors to enhance the downscaling performance of satellite precipitation data can explore the following avenues: First, investigating precipitation data downscaling through the

use of multielement satellite data fusion methods should be considered to address challenges related to the inherent data quality of satellite data itself [24]. Second, the current focus on constructing GWRK precipitation downscaling models primarily at annual and monthly scales could be extended. There is potential to develop GWRK models at finer time resolutions, such as ten-day, daily, or even hourly scales. Exploring the application of GWRK or alternative downscaling methods at these finer time scales will better align with the requirements of relevant scientific research [64], [65]. Finally, investigating novel downscaling algorithms, such as artificial neural networks, and integrating multiple downscaling models can contribute to obtaining more accurate and reliable high spatial resolution precipitation data [66].

VII. Conclusion

This study developed a monthly scale GWRK precipitation downscaling model in the Songhua River Basin. Utilizing the correlation between environmental variables, i.e., DEM, slope, LST, soil moisture, and precipitation, the model downscaled precipitation data from 0.1° to 1 km spatial resolution. Subsequently, the monthly scale data underwent decomposition into daily scale data through the daily fraction method and GDA method, with the integration of rain gauge data for calibration and verification of the daily scale data. Ultimately, long-term high-quality daily data were obtained. This methodology was applied to examine spatiotemporal changes in monthly and daily precipitation in the Songhua River Basin from 2001 to 2020.

The research findings indicate that the GWRK precipitation downscaling model yielded favorable outcomes owing to the strong correlation between spatial auxiliary variables and precipitation. The CC value of the downscaled monthly precipitation data increased to 0.966, a rise of 1.4%. Furthermore, high-quality monthly scale data were transformed to the daily scale (1 km) through the original satellite data's daily fraction scaling. The CC value of the downscaled daily precipitation data reached 0.772, a 3.9% improvement compared with the original daily data. To further enhance data quality, rain gauge data integration was conducted using the GDA method to calibrate and verify the downscaled daily data. The final results demonstrated that data calibrated by integrating rain gauge data achieved optimal downscaling results (CC = 0.818, RMSE = 3.188, and ME = 0.086).

Additionally, spatiotemporal analysis of annual-scale precipitation revealed a noticeable upward trend in the Songhua River Basin during the study period (2001–2020). This trend gradually intensified from the Greater Khingan Range toward the east and west.

In summary, the proposed GWRK precipitation downscaling model, integrating precipitation with environmental variables of DEM, slope, LST, and soil moisture, exhibits robust applicability in the Songhua River Basin.

Acknowledgment

The authors would like to thank the Space-Time Tripolar Environmental Big Data Platform (https://doi.org/10.11888/Terre.tpdc.272415), the National Aeronautics and Space Administration (NASA), and the China Meteorological Administration (CMA) (http://data.cma.cn) for providing datasets. The comments from reviewers have considerably improved the quality of the work presented here.

References

[1] S. Jia, W. Zhu, A. Lű, and T. Yan, "A statistical spatial downscaling algorithm of TRMM precipitation based on NDVI and DEM in the Qaidam Basin of China," *Remote Sens. Environ.*, vol. 115, no. 12, pp. 3069–3079, Dec. 2011, doi: 10.1016/j.rse.2011.06.009.

[2] Z. Duan and W. G. M. Bastiaanssen, "First results from version 7 TRMM 3B43 precipitation product in combination with a new downscaling–calibration procedure," *Remote Sens. Environ.*, vol. 131, pp. 1–13, Apr. 2013, doi: 10.1016/j.rse.2012.12.002.

[3] T. Zhang, Y. Yang, Z. Dong, and S. Gui, "A multiscale assessment of three satellite precipitation products (TRMM, CMORPH, and PERSIANN) in the three Gorges reservoir area in China," *Adv. Meteorol.*, vol. 2021, Jun. 2021, Art. no. e9979216, doi: 10.1155/2021/9979216.

[4] N. Bijaber et al., "Developing a remotely sensed drought monitoring indicator for Morocco," *Geosciences*, vol. 8, no. 2, Feb. 2018, Art. no. 55, doi: 10.3390/geosciences8020055.

[5] J. Fang, J. Du, W. Xu, P. Shi, M. Li, and X. Ming, "Spatial downscaling of TRMM precipitation data based on the orographical effect and meteorological conditions in a mountainous area," *Adv. Water Resour.*, vol. 61, pp. 42–50, Nov. 2013, doi: 10.1016/j.advwatres.2013.08.011.

[6] H. Wang, F. Zang, C. Zhao, and C. Liu, "A GWR downscaling method to reconstruct high-resolution precipitation dataset based on GSMaP-gauge data: A case study in the Qilian Mountains, Northwest China," *Sci. Total Environ.*, vol. 810, Mar. 2022, Art. no. 152066, doi: 10.1016/j.scitotenv.2021.152066.

[7] Z. Zhou, B. Guo, W. Xing, J. Zhou, F. Xu, and Y. Xu, "Comprehensive evaluation of latest GPM era IMERG and GSMaP precipitation products over mainland China," *Atmos. Res*, vol. 246, Dec. 2020, Art. no. 105132, doi: 10.1016/j.atmosres.2020.105132.

[8] Y. Chen et al., "A new downscaling-integration framework for high-resolution monthly precipitation estimates: Combining rain gauge observations, satellite-derived precipitation data and geographical ancillary data," *Remote Sens. Environ.*, vol. 214, pp. 154–172, Sep. 2018, doi: 10.1016/j.rse.2018.05.021.

[9] S. I. Bohnenstengel, K. H. Schlünzen, and F. Beyrich, "Representativity of in situ precipitation measurements—A case study for the LITFASS area in North-Eastern Germany," *J. Hydrol.*, vol. 400, no. 3, pp. 387–395, Apr. 2011, doi: 10.1016/j.jhydrol.2011.01.052.

[10] L. Chao, K. Zhang, Z. Li, Y. Zhu, J. Wang, and Z. Yu, "Geographically weighted regression based methods for merging satellite and gauge precipitation," *J. Hydrol.*, vol. 558, pp. 275–289, Mar. 2018, doi: 10.1016/j.jhydrol.2018.01.042.

[11] C. Massari, W. Crow, and L. Brocca, "An assessment of the performance of global rainfall estimates without ground-based observations," *Hydrol. Earth Syst. Sci.*, vol. 21, no. 9, pp. 4347–4361, Sep. 2017, doi: 10.5194/hess-21-4347-2017.

[12] R. Celleri, P. Willems, W. Buytaert, and J. Feyen, "Space–time rainfall variability in the Paute basin, Ecuadorian Andes," *Hydrol. Process.*, vol. 21, no. 24, pp. 3316–3327, 2007, doi: 10.1002/hyp.6575.

[13] A. Barbulescu, "A new method for estimation the regional precipitation," *Water Resour. Manage.*, vol. 30, no. 1, pp. 33–42, Jan. 2016, doi: 10.1007/s11269-015-1152-2.

[14] S. Jiang et al., "Comprehensive evaluation of multi-satellite precipitation products with a dense rain gauge network and optimally merging their simulated hydrological flows using the Bayesian model averaging method," *J. Hydrol.*, vol. 452–453, pp. 213–225, Jul. 2012, doi: 10.1016/j.jhydrol.2012.05.055.

[15] S. Xu, C. Wu, L. Wang, A. Gonsamo, Y. Shen, and Z. Niu, "A new satellite-based monthly precipitation downscaling algorithm with non-stationary relationship between precipitation and land surface characteristics," *Remote Sens. Environ.*, vol. 162, pp. 119–140, Jun. 2015, doi: 10.1016/j.rse.2015.02.024.

[16] A. Abdollahipour, H. Ahmadi, and B. Aminnejad, "A review of downscaling methods of satellite-based precipitation estimates," *Earth Sci. Inform.*, vol. 15, no. 1, pp. 1–20, Mar. 2022, doi: 10.1007/s12145-021-00669-4.

[17] G. J. Huffman et al., "The global precipitation climatology project (GPCP) combined precipitation dataset," *Bull. Amer. Meteorol. Soc.*, vol. 78, no. 1, pp. 5–20, Jan. 1997, doi: 10.1175/1520-0477(1997)078<0005:TGPCPG>2.0.CO;2.

[18] Y. Jing, L. Lin, X. Li, T. Li, and H. Shen, "An attention mechanism based convolutional network for satellite precipitation downscaling over China," *J. Hydrol.*, vol. 613, Oct. 2022, Art. no. 128388, doi: 10.1016/j.jhydrol.2022.128388.

[19] T. Kubota et al., "Global precipitation map using satellite-borne microwave radiometers by the GSMaP project: Production and validation," *IEEE Trans. Geosci. Remote Sens.*, vol. 45, no. 7, pp. 2259–2275, Jul. 2007, doi: 10.1109/TGRS.2007.895337.

[20] C. Kummerow, W. Barnes, T. Kozu, J. Shiue, and J. Simpson, "The tropical rainfall measuring mission (TRMM) sensor package," *J. Atmos. Ocean. Technol.*, vol. 15, no. 3, pp. 809–817, Jun. 1998, doi: 10.1175/1520-0426(1998)015<0809:TTRMMT>2.0.CO;2.

[21] M. Xu et al., "PreciPatch: A dictionary-based precipitation downscaling method," *Remote Sens.*, vol. 12, no. 6, Jan. 2020, Art. no. 1030, doi: 10.3390/rs12061030.

[22] A. Arshad et al., "Reconstructing high-resolution gridded precipitation data using an improved downscaling approach over the high altitude mountain regions of Upper Indus Basin (UIB)," *Sci. Total Environ.*, vol. 784, Aug. 2021, Art. no. 147140, doi: 10.1016/j.scitotenv.2021.147140.

[23] A. H. Nury, A. Sharma, L. Marshall, and R. Mehrotra, "Characterising uncertainty in precipitation downscaling using a Bayesian approach," *Adv. Water Resour.*, vol. 129, pp. 189–197, Jul. 2019, doi: 10.1016/j.advwatres.2019.05.018.

[24] C. Xu, C. Liu, W. Zhang, Z. Li, and B. An, "Downscaling and merging of daily scale satellite precipitation data in the Three River headwaters region fused with cloud attributes and rain gauge data," *Water*, vol. 15, no. 6, Jan. 2023, Art. no. 1233, doi: 10.3390/w15061233.

[25] E. Sharifi, B. Saghafian, and R. Steinacker, "Downscaling satellite precipitation estimates with multiple linear regression, artificial neural networks, and spline interpolation techniques," *J. Geophys. Res. Atmos.*, vol. 124, no. 2, pp. 789–805, Jan. 2019, doi: 10.1029/2018JD028795.

[26] H. Zhu, H. Liu, Q. Zhou, and A. Cui, "A XGBoost-based downscaling-calibration scheme for extreme precipitation events," *IEEE Trans. Geosci. Remote Sens.*, vol. 61, pp. 1–12, 2023, Art. no. 4103512, doi: 10.1109/TGRS.2023.3294266.

[27] Y. Jing, L. Lin, X. Li, T. Li, and H. Shen, "Cascaded downscaling–Calibration networks for satellite precipitation estimation," *IEEE Geosci. Remote Sens. Lett.*, vol. 19, pp. 1–5, 2022, Art. no. 1506105, doi: 10.1109/LGRS.2022.3214083.

[28] C. Chen, S. Zhao, Z. Duan, and Z. Qin, "An improved spatial downscaling procedure for TRMM 3B43 precipitation product using geographically weighted regression," *IEEE J. Sel. Topics Appl. Earth Observ. Remote Sens.*, vol. 8, no. 9, pp. 4592–4604, Sep. 2015, doi: 10.1109/JSTARS.2015.2441734.

[29] Z. Ma, Y. Zhou, B. Hu, Z. Liang, and Z. Shi, "Downscaling annual precipitation with TMPA and land surface characteristics in China," *Int. J. Climatol.*, vol. 37, no. 15, pp. 5107–5119, 2017, doi: 10.1002/joc.5148.

[30] A. Retalis, F. Tymvios, D. Katsanos, and S. Michaelides, "Downscaling CHIRPS precipitation data: An artificial neural network modelling approach," *Int. J. Remote Sens.*, vol. 38, no. 13, pp. 3943–3959, Jul. 2017, doi: 10.1080/01431161.2017.1312031.

[31] S. Chen, L. Xiong, Q. Ma, J.-S. Kim, J. Chen, and C.-Y. Xu, "Improving daily spatial precipitation estimates by merging gauge observation with multiple satellite-based precipitation products based on the geographically weighted ridge regression method," *J. Hydrol.*, vol. 589, Oct. 2020, Art. no. 125156, doi: 10.1016/j.jhydrol.2020.125156.

[32] B. Liu et al., "Chemical weathering under mid- to cool temperate and monsoon-controlled climate: A study on water geochemistry of the Songhuajiang River system, northeast China," *Appl. Geochem.*, vol. 31, pp. 265–278, Apr. 2013, doi: 10.1016/j.apgeochem.2013.01.015.

[33] Y. Gao et al., "Characterizing legacy nitrogen-induced time lags in riverine nitrogen reduction for the Songhuajiang River Basin: Source analysis, spatio-seasonal patterns, and impacts on future water quality improvement," *Water Res.*, vol. 242, Aug. 2023, Art. no. 120292, doi: 10.1016/j.watres.2023.120292.

[34] B. Su, X. Zeng, J. Zhai, Y. Wang, and X. Li, "Projected precipitation and streamflow under SRES and RCP emission scenarios in the Songhuajiang River basin, China," *Quaternary Int.*, vol. 380–381, pp. 95–105, Sep. 2015, doi: 10.1016/j.quaint.2014.03.049.

[35] Y. Cheng et al., "Spatial and temporal stability of temperature in the first-level basins of China during 1951–2013," *Theor. Appl. Climatol.*, vol. 136, no. 3, pp. 863–874, May 2019, doi: 10.1007/s00704-018-2522-5.

[36] X. Li, C. Wellen, G. Liu, Y. Wang, and Z.-L. Wang, "Estimation of nutrient sources and transport using spatially referenced regressions on watershed attributes: A case study in Songhuajiang River Basin, China," *Environ. Sci. Pollut. Res.*, vol. 22, no. 9, pp. 6989–7001, May 2015, doi: 10.1007/s11356-014-3903-7.

[37] F. Aslami, A. Ghorbani, B. Sobhani, and A. Esmali, "Comprehensive comparison of daily IMERG and GSMaP satellite precipitation products in Ardabil Province, Iran," *Int. J. Remote Sens.*, vol. 40, no. 8, pp. 3139–3153, Apr. 2019, doi: 10.1080/01431161.2018.1539274.

[38] M. L. Tan and H. Santo, "Comparison of GPM IMERG, TMPA 3B42 and PERSIANN-CDR satellite precipitation products over Malaysia," *Atmos. Res*, vol. 202, pp. 63–76, Apr. 2018, doi: 10.1016/j.atmosres.2017.11.006.

[39] J. Fang, W. Yang, Y. Luan, J. Du, A. Lin, and L. Zhao, "Evaluation of the TRMM 3B42 and GPM IMERG products for extreme precipitation analysis over China," *Atmos. Res*, vol. 223, pp. 24–38, Jul. 2019, doi: 10.1016/j.atmosres.2019.03.001.

[40] Dashan Wang, X. Wang, L. Liu, D. Wang, H. Huang, and C. Pan, "Evaluation of TMPA 3B42V7, GPM IMERG and CMPA precipitation estimates in Guangdong Province, China," *Int. J. Climatol.*, vol. 39, no. 2, pp. 738–755, 2019, doi: 10.1002/joc.5839.

[41] Z. Zhang, J. Tian, Y. Huang, X. Chen, S. Chen, and Z. Duan, "Hydrologic evaluation of TRMM and GPM IMERG satellite-based precipitation in a humid basin of China," *Remote Sens.*, vol. 11, no. 4, Jan. 2019, Art. no. 431, doi: 10.3390/rs11040431.

[42] Q. Li et al., "A 1 km daily soil moisture dataset over China using in situ measurement and machine learning," *Earth Syst. Sci. Data*, vol. 14, no. 12, pp. 5267–5286, Nov. 2022, doi: 10.5194/essd-14-5267-2022.

[43] W. Shangguan, Q. Li, and G. Shi, "A 1-km daily soil moisture dataset over China based on in situ measurement (2000–2020)," National Tibetan Plateau Data Center, 2022, doi: 10.11888/Terre.tpdc.272415https://cstr.cn/18406.11.Terre.tpdc.272415.

[44] C. Brunsdon, A. S. Fotheringham, and M. E. Charlton, "Geographically weighted regression: A method for exploring spatial nonstationarity," *Geograph. Anal.*, vol. 28, no. 4, pp. 281–298, Oct. 1996, doi: 10.1111/j.1538-4632.1996.tb00936.x.

[45] G. M. Foody, "Geographical weighting as a further refinement to regression modelling: An example focused on the NDVI–rainfall relationship," *Remote Sens. Environ.*, vol. 88, no. 3, pp. 283–293, Dec. 2003, doi: 10.1016/j.rse.2003.08.004.

[46] N. Zhao et al., "Statistical downscaling of precipitation using local regression and high accuracy surface modeling method," *Theor. Appl. Climatol.*, vol. 129, no. 1, pp. 281–292, Jul. 2017, doi: 10.1007/s00704-016-1776-z.

[47] W. Simeng, W. Dazhao, and H. Chang, "A comparative study of using ANUSPLIN and GWR models for downscaled GPM precipitation," in *Proc. 8th Int. Conf. Agro-Geoinform.*, Jul. 2019, pp. 1–5, doi: 10.1109/Agro-Geoinformatics.2019.8820704.

[48] A. Karbalaye Ghorbanpour, T. Hessels, S. Moghim, and A. Afshar, "Comparison and assessment of spatial downscaling methods for enhancing the accuracy of satellite-based precipitation over Lake Urmia Basin," *J. Hydrol.*, vol. 596, May 2021, Art. no. 126055, doi: 10.1016/j.jhydrol.2021.126055.

[49] Y. Gao, J. Huang, Shuang Li, and S. Li, "Spatial pattern of non-stationarity and scale-dependent relationships between NDVI and climatic factors—A case study in Qinghai-Tibet Plateau, China," *Ecol. Indicators*, vol. 20, pp. 170–176, Sep. 2012, doi: 10.1016/j.ecolind.2012.02.007.

[50] A. S. Fotheringham, C. Brunsdon, and M. Charlton, *Geographically Weighted Regression: The Analysis of Spatially Varying Relationships*. Hoboken, NJ, USA: Wiley, 2003.

[51] M. J. M. Cheema and W. G. M. Bastiaanssen, "Local calibration of remotely sensed rainfall from the TRMM satellite for different periods and spatial scales in the Indus Basin," *Int. J. Remote Sens.*, vol. 33, no. 8, pp. 2603–2627, Apr. 2012, doi: 10.1080/01431161.2011.617397.

[52] M. Li and Q. Shao, "An improved statistical approach to merge satellite rainfall estimates and raingauge data," *J. Hydrol.*, vol. 385, no. 1/4, pp. 51–64, May 2010, doi: 10.1016/j.jhydrol.2010.01.023.

[53] W. W. Immerzeel, M. M. Rutten, and P. Droogers, "Spatial downscaling of TRMM precipitation using vegetative response on the Iberian Peninsula," *Remote Sens. Environ.*, vol. 113, no. 2, pp. 362–370, Feb. 2009, doi: 10.1016/j.rse.2008.10.004.

[54] Q. He, T. Yang, B. Liu, and S. Zhou, "Study on the satellite-based precipitation downscaling algorithm in Tianshan mountain," in *Proc. IEEE Int. Geosci. Remote Sens. Symp.*, 2016, pp. 605–608, doi: 10.1109/IGARSS.2016.7729151.

[55] H. Zhang, H. A. Loáiciga, D. Ha, and Q. Du, "Spatial and temporal downscaling of TRMM precipitation with novel algorithms," *J. Hydrometeorol.*, vol. 21, no. 6, pp. 1259–1278, Jun. 2020, doi: 10.1175/JHM-D-19-0289.1.
[56] H. Zhu and Q. Zhou, "Advancing satellite-derived precipitation downscaling in data-sparse area through deep transfer learning," *IEEE Trans. Geosci. Remote Sens.*, vol. 62, pp. 1–13, 2024, Art. no. 4102513, doi: 10.1109/TGRS.2024.3367332.
[57] H. Zhu, H. Liu, Q. Zhou, and A. Cui, "Towards an accurate and reliable downscaling scheme for high-spatial-resolution precipitation data," *Remote Sens.*, vol. 15, no. 10, May 2023, Art. no. 2640, doi: 10.3390/rs15102640.
[58] A. AghaKouchak, A. Behrangi, S. Sorooshian, K. Hsu, and E. Amitai, "Evaluation of satellite-retrieved extreme precipitation rates across the central United States," *J. Geophys. Res. Atmos.*, vol. 116, no. D2, 2011, Art. no. D02115, doi: 10.1029/2010JD014741.
[59] C. Kidd, D. R. Kniveton, M. C. Todd, and T. J. Bellerby, "Satellite rainfall estimation using combined passive microwave and infrared algorithms," *J. Hydrometeorol.*, vol. 4, no. 6, pp. 1088–1104, Dec. 2003, doi: 10.1175/1525-7541(2003)004< 1088:SREUCP >2.0.CO;2.
[60] M. Girons Lopez, H. Wennerström, L. Nordén, and J. Seibert, "Location and density of rain gauges for the estimation of spatial varying precipitation," *Geografiska Ann., Ser. A, Phys. Geogr.*, vol. 97, no. 1, pp. 167–179, Mar. 2015, doi: 10.1111/geoa.12094.
[61] H. McMillan, T. Krueger, and J. Freer, "Benchmarking observational uncertainties for hydrology: Rainfall, river discharge and water quality," *Hydrol. Process.*, vol. 26, no. 26, pp. 4078–4111, 2012, doi: 10.1002/hyp.9384.
[62] K. Sugiura, D. Yang, and T. Ohata, "Systematic error aspects of gauge-measured solid precipitation in the Arctic, Barrow, Alaska," *Geophys. Res. Lett.*, vol. 30, no. 4, 2003, Art. no. 1192, doi: 10.1029/2002GL015547.
[63] D. Yang, D. Kane, Z. Zhang, D. Legates, and B. Goodison, "Bias corrections of long-term (1973–2004) daily precipitation data over the northern regions," *Geophys. Res. Lett.*, vol. 32, no. 19, 2005, Art. no. L19501, doi: 10.1029/2005GL024057.
[64] Z. Ma et al., "An updated moving window algorithm for hourly-scale satellite precipitation downscaling: A case study in the Southeast Coast of China," *J. Hydrol.*, vol. 581, Feb. 2020, Art. no. 124378, doi: 10.1016/j.jhydrol.2019.124378.
[65] Y. Shen, P. Zhao, Y. Pan, and J. Yu, "A high spatiotemporal gauge-satellite merged precipitation analysis over China," *J. Geophys. Res. Atmos.*, vol. 119, no. 6, pp. 3063–3075, 2014, doi: 10.1002/2013JD020686.
[66] M. H. Ribeiro Sales, C. M. Souza, and P. C. Kyriakidis, "Fusion of MODIS images using kriging with external drift," *IEEE Trans. Geosci. Remote Sens.*, vol. 51, no. 4, pp. 2250–2259, Apr. 2013, doi: 10.1109/TGRS.2012.2208467.

Bo Zhang received the M.S. degree in environmental science from Northeast Forestry University, Harbin, China, in 2014.

She currently serves as the General Manager of Environmental Construction Ecological Restoration (Beijing) Co., Ltd., Beijing, China, and a Senior Engineer of the Chinese Academy of Environmental Sciences, Beijing, and the Institute of Lake Ecology and Environment. Her research direction is mainly water environment pollution control and restoration.

Chuanqi Liu received the B.S. degree in surveying and mapping engineering from the Lanzhou University of Technology, Lanzhou, China, in 2020. He is currently working toward the Ph.D. degree in cartography and geographic information systems with the Institute of Aerospace Information Innovation, Chinese Academy of Sciences, Beijing, China.

His research interests mainly include multisource remote sensing data analysis, and watershed hydrology and water quality model construction and analysis, etc.

Zhijie Zhang received the B.S. degree in electrical engineering and automation from the Nanjing University of Post and Telecommunications, Nanjing, China, in 2014, the M.S. degree in computer engineering from Rutgers University, New Brunswick, NJ, USA, in 2018, and the Ph.D. degree in remote sensing and GIS in geography from the University of Connecticut, Storrs, CT, USA, in 2022.

During his academic pursuit, he engaged in valuable research experiences. From 2016 to 2017, he was a research student with WINLAB, Rutgers, NJ, USA, where he contributed to two Internet of Things sensor network projects. Subsequently, from 2018 to 2022, he was a Research Assistant with Geography Department, University of Connecticut. Since 2022, he has been in the position of Postdoctoral Research Associate with the School of Geography, Development and Environment, The University of Arizona, Tucson, AZ, USA. He currently serves as an Assistant Professor with the Department of Environment and Society, Quinney College of Natural Resources, Utah State University, Logan, UT, USA. His research interests primarily revolve around the application of deep learning methods in various domains, including remote sensing, hydrology studies, and landslide and flood disaster studies.

Shengqing Xiong received the B.Sc. degree in hydrogeology and engineering geology from the Chengdu College of Geology (now the Chengdu University of Science and Technology), Chengdu, China, in 1983, and the Ph.D. degree in applied geophysics from the China University of Geosciences, Beijing, China, in 1997.

He holds several esteemed positions within academia and professional societies. He serves as a member of the Expert Advisory Committee of the Ministry of Land and Resources, as well as a member of the Higher Education Teaching Steering Committee of the Ministry of Education. Additionally, he is a Doctoral Supervisor with the School of Geological Engineering and Surveying and Mapping, Chang'an University, Xi'an, China, and holds special Professor and Doctoral Supervisor positions with the China University of Geosciences and the Chengdu University of Science and Technology. Furthermore, he is the Vice-President of the Geophysics Society of China, a member of the Council of the China Society of Geosciences, and an Editor-in-Chief for "Physical Prospecting and Chemistry." His research focuses on theoretical and applied studies of airborne geophysical survey methods and techniques. He has authored 18 monographs, authored or coauthored more than 100 papers, and held 5 patents. His research interests include but are not limited to theoretical and applied research on airborne geophysical survey methods and technologies.

Dr. Xiong was a recipient of one special prize and two second prizes of the National Science and Technology Progress Award, and has been recognized for his contributions.

Wanchang Zhang received the first M.S. degree in geography from The Cold and Arid Regions Environmental and Engineering Research Institute, Chinese Academy of Sciences (CAS), Lanzhou, China, in 1992, the second M.S. degree in hydrospheric–atmospheric science through IHAS Special Program sponsored by UNESCO from Nagoya University, Nagoya, Japan, in 1996, and the Ph.D. degree in Earth system science from the Department of Earth and Planetary Sciences, Graduate School of Science, Nagoya University, Nagoya, in 2000.

He is a distinguished member of the IEEE and holds a diverse educational background and extensive experience in the field of Earth system science. Upon completing his doctoral studies, he returned to China and assumed the position of a Full Professor and the Ph.D. Supervisor with the International Institute of Earth System Science, Nanjing University. In 2005, he was promoted under the prestigious "100 Talent Researcher Program" sponsored by CAS, Beijing in 2005, focusing on his research on global changes with the Institute for Atmospheric Physics, CAS, Beijing. Since 2012, he has been affiliated with Aerospace Information Research Institute, CAS, Beijing. His research interests encompass various aspects of remote sensing (RS) and geographic information systems (GISs) applications in Earth system sciences. Specifically, he specializes in the integration of RS and GIS technologies to develop distributed ecohydro-climatic models for hydrology, water resources, and environmental studies. Additionally, his expertise extends to global disaster and environmental studies, utilizing RS and GIS techniques in conjunction with modeling schemes.

Zhenghao Li received the bachelor's degree in surveying and mapping engineering from the School of Earth Sciences and Engineering, Hohai University, Nanjing, China, in 2021. He is currently working toward the Ph.D. degree in cartography and geographic information systems with the Key Laboratory of Digital Earth Sciences, Aerospace Information Research Institute, Chinese Academy of Sciences, Beijing, China.

His research interests include remote sensing, hydrology, and machine learning.

Bangsheng An received the B.S. degree in geophysics from the China University of Mining and Technology, Beijing, China, in 2021. He is currently working toward the Ph.D. degree in cartography and GIS with Aerospace Information Research Institute, Chinese Academy of Sciences, Beijing.

His research interests include deep learning, geohazard monitoring, and risk assessment.

Shuhang Wang received the M.S. degree in environmental science from the Hefei University of Technology, Hefei, China, in 2014.

He is currently the Director of the National Engineering Laboratory for Lake Pollution Control and Ecological Restoration, Chinese Research Academy of Environmental Sciences, Beijing, China. His research directions mainly include but are not limited to migration and transformation of pollutants at the water-sediment interface, sediment pollution control and resource utilization, and river and lake water ecological protection and restoration.